

Title	Determination of Micro-reactor Volume from the Transient Concentration Profile by Means of a Time-of-Flight Mass Spectrometer and the Application to the Rate Constant Measurement of Fast Reactions, O+NO NO+O and N+NO N +O
Author(s)	Takezaki, Yoshimasa; Mori, Sadayuki
Citation	Bulletin of the Institute for Chemical Research, Kyoto University (1968), 45(6): 388-405
Issue Date	1968-03-30
URL	<a href="http://hdl.handle.net/2433/76220">http://hdl.handle.net/2433/76220</a>
Right	
Type	Departmental Bulletin Paper
Textversion	publisher

# Determination of Micro-reactor Volume from the Transient Concentration Profile by Means of a Time-of-Flight Mass Spectrometer and the Application to the Rate Constant Measurement of Fast Reactions, $O + NO_2 \rightarrow NO + O_2$ and $N + NO \rightarrow N_2 + O^*$

Yoshimasa TAKEZAKI and Sadayuki MORI\*\*

(Takezaki Laboratory)

Received December 24, 1967

A new method has been developed in measuring the rate constant of very fast atom-reaction in a fast flow system with a complete mixing micro-reactor (residence time *ca.* 1 msec).

The effective volume of the reaction zone (*ca.* 2 cc) is determined from the transient concentration profile of atoms in the effluent carrier gas out of the reactor observed without the second reactant by means of a time-of-flight mass spectrometer over 10 msec with 25  $\mu$ sec intervals, where the incoming atoms are produced in bunches with sharp fronts by the square pulses of microwave discharge.

From the effective volume thus obtained, the steady concentration ratios of atom between those before and after the reaction, and the concentration of the second reactant which leaves the reactor, both determined mass spectrometrically in the effluent gas, the rate constant of fast bimolecular elementary reaction can be calculated.

This procedure has been examined by the well-known fast reaction  $NO_2 + O \rightarrow NO + O_2$   $k \approx 3 \times 10^9$  l/mole·sec at 300°K and  $N + NO \rightarrow N_2 + O$   $k \approx 2 \times 10^{10}$  at room temperature as examples; the observed rate constants are  $(4.2 \pm 0.6) \times 10^9$  at 30°C and  $(1.1 \pm 0.14) \times 10^{10}$  near room temperature, respectively, in fair agreement with the reported values.

Although this method is not yet satisfactory in precision at the present stage it appears to have a potential applicability in this field.

## I. INTRODUCTION

In the kinetic study of free radical reaction by means of a mass spectrometer in flow system, measurements of the steady concentrations of the components sampled at the end of the flow line of definite lengths from the mixing point have been usually performed. In some cases the stirred tank reactor techniques have been also used.<sup>1,2)</sup> In both methods, however, especially in the latter, a difficult problem may arise in the analysis of the results when it is to be applied to the very fast reaction,<sup>1)</sup> *e.g.*,  $k \geq 10^9$  l/mole·sec; it would happen that the residence time in the reactor has to be reduced to get appropriate con-

\* This paper was read at the International Conference on Photochemistry 1967, München (except the last chapter), and also at the Second Symposium on Fast Reactions, 1967, Kyoto, Japan.

\*\* 竹崎 嘉眞, 森 貞之

## Determination of Micro-reactor Volume by TOF Mass Spectrometer

versions while the concentrations of active species are maintained rather high in order to obtain accurate determinations, and this short residence time becomes close to the time of diffusion and makes the simple stirred reactor treatment hardly applicable. Further, owing to the practical limitation to raise the flow speed extremely, the volume of the reactor should be diminished and, although this has an advantage in making a fast and complete mass mixing of the two reactants easy the precise estimation of actual residence time appears to become difficult because the uncalculable uncertainty of the reaction zone caused by the complexity of the reactor geometry and the interspace to the leak of the mass spectrometer comes appreciably into the effective reaction volume.

In an attempt to overcome this hurdle in the stirred reactor experiment, an alternative procedure has been developed to estimate the effective volume which may be tentatively usable in the analysis, based on the measurement of transient change of the concentration of radicals in the effluent gas from a micro-reactor, where the observation being made by a time-of-flight mass spectrometer.

Then, the capability of this method has been checked by the well-known fast reaction  $O + NO_2 \rightarrow O_2 + NO$  and  $N + NO \rightarrow N_2 + O$  as examples. At the present stage the result is not so satisfactory in precision, and there remain weak points to be refined in theory and technique, but it seems that this idea has a fair applicability in this field.

## II. PRINCIPLE AND MEASURING SYSTEM

A bunch of atoms of one kind with a constant concentration  $C_0$  and a sharp front is produced by means of square form micro-wave discharge acting on a small amount of atom-source molecules contained in a fast stream of a carrier gas, the stream then enters into a micro-reactor and the second reactant is introduced there through another port, meanwhile the pin hole of TOF mass spectrometer opens closest to the outlet hole of the reactor connected with a high speed vacuum line (Fig. 1).

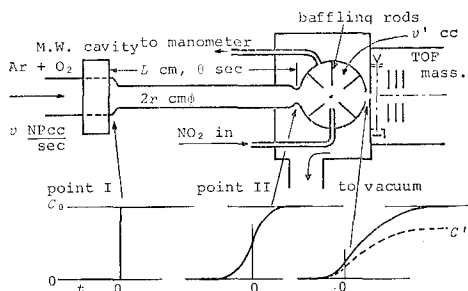


Fig. 1. Reaction system and the atom concentration profile.

Now, under the condition that the radial diffusion of atoms in the inlet tube is very fast to equalize the radial distribution caused by the velocity gradient in the laminar flow of the carrier gas during the passage from the M.W. cavity (point I) to the reactor entrance (point II), which is realizable as shown later,

only the axial diffusion should be considered as the cause of the downstream deformation of sharp front, therefore the profile of atom concentration at the point II is given by eq. 1, and if the *instant* and *perfect* mixing occurs in the reactor, the feature of atom concentration in the effluent gas should be expressed by eq. 2, in the absence of the second reactant.

$$C/C_0 = \frac{1}{2} \{1 + \operatorname{erf}(t/x)\}^* \quad (1)$$

$$C/C_0 = \frac{\alpha_1}{2\alpha_2} \left[ 1 + \operatorname{erf}(t/x) - \left\{ 1 + \operatorname{erf}\left(\frac{t}{x} - \frac{x\alpha_2}{2}\right) \right\} \exp\left(\frac{\alpha_2^2 x^2}{4} - \alpha_2 t\right) \right] \quad (2)$$

$$x = (4\bar{D}\theta)^{1/2}/\bar{U} = 3.07 \times 10^{-4} (D'L/v^3)^{1/2} r^3 p_1 \left\{ \frac{1 - \left(1 - \frac{\beta L}{p_1^2}\right)^{3/2}}{1 - \left(1 - \frac{\beta L}{p_1^2}\right)^{1/2}} \right\}^{1/2} \quad (3)$$

where

$C$  volumetric mean concentration of atoms

$t$  time of observation, sec (+ or - ; origin is the hypothetical time of arrival of the front at the point II assuming no axial diffusion)

$\alpha_1$  space velocity of atom-carrier gas =  $760 v/v' p_{reactor}$ , sec<sup>-1</sup>

$\alpha_2$  space velocity of total gas = (total gas volumetric flow rate at the reactor pressure)  $\div v'$ , sec<sup>-1</sup>

$v$  atom-carrier gas flow rate, NPcc/sec

$v'$  effective volume of the reaction zone, cc

$p$  static pressure of gas, mmHg

$\bar{D}$  mean (between points I and II) diffusion coefficient of atom, cm<sup>2</sup>/sec

$D'$  diffusion coefficient of atom at 1 mmHg, cm<sup>2</sup>·mmHg/sec

$L$  distance between points I and II, cm

$\theta$  actual time of transit between I and II, sec

$\bar{U}$  mean (radial and between I and II) linear velocity of carrier gas, cm/sec

$r$  inner radius of the carrier gas flow tube between I and II, cm

$\beta$   $16\mu U_1 p_1 / 1330 r^2 = 2.91 \mu v / r^4$

$\mu$  viscosity of carrier gas, poise

subscript 0 represents the original quantity.

In the derivation of eq. 3 integral averages of gradually changing  $U$  and  $D$  due to the pressure drop have been used. Thus, if we can find a parameter  $v'$  which makes the calculated curve of eq. 2 coincide with the observed one over the entire range, this must give the effective reaction volume within which the complete mixing is regarded to take place under the specified flow condition and the reactor construction.

Next, when the second reactant  $B$  (diluted with the carrier gas if necessary) is introduced and if the elementary reaction occurring is solely the bimolecular elementary step "atom +  $B$ ", the concentration of atoms in the effluent gas

\* Strictly speaking,  $\chi$  should be  $\sqrt{4\bar{D}(t+\theta)/\bar{U}}$ , instead of  $\sqrt{4\bar{D}\theta/\bar{U}}$  given in the text. However, it can be shown that under the present experimental conditions shown later the omission of  $t$  causes only negligible deviation from the correct one, therefore for simplicity in the subsequent calculation we are to use this simplified  $t$ -independent parameter.

Determination of Micro-reactor Volume by TOF Mass Spectrometer

$C'$  should be reduced to

$$\frac{C'}{C_0} = \frac{\alpha_1}{\alpha_2} \cdot \frac{\alpha_2}{\alpha_2 + k(B_0)(B/B_0)} \quad (4)$$

for the sufficiently large  $t$ . The observed quantities  $C'/C_0$ ,  $\alpha_1$ ,  $\alpha_2$ ,  $(B_0)$  and  $(B/B_0)$  enable us to calculate the absolute value of that rate constant  $k$ .

In order to observe concentration profiles, some trigger, delay and gate circuits have been added to a TOF mass spectrometer (modified to act at 40 kc) together with a modulator of M.W. power input system to produce square waves, all being synchronized with the main pulse of the mass spectrometer (Fig. 2). By this means we can observe a number of one specified mass peak displays,

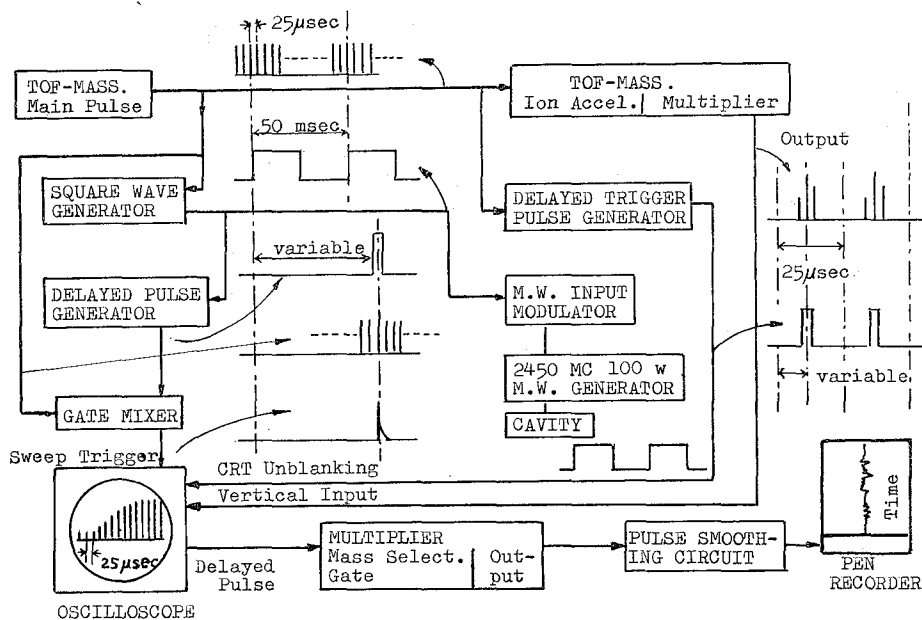


Fig. 2. Block diagram of measuring system.

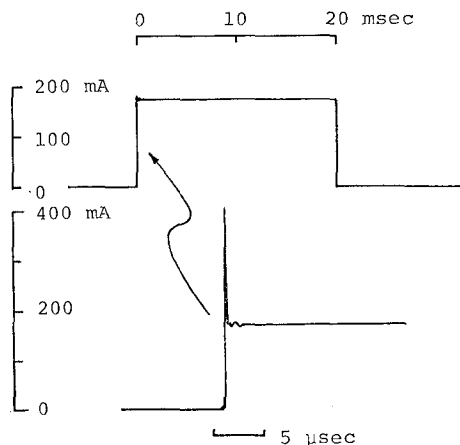


Fig. 3. Form of M.W. square wave.

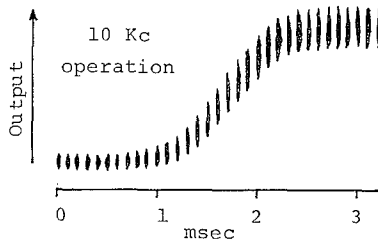


Fig. 4. Photogram of oscilloscope display (schematic).

appearing once a mass spectrometer cycle ( $25 \mu\text{sec}$  interval) and changing successively along a relatively slow sweep ( $5 \text{ msec/cm}$ ) started by the rise of M.W. square input with any desired delay time. The observed shape of the M.W. input is represented schematically in Fig. 3; the rise time and the flatness of the plateau are satisfactory for the present study.

As is well known, the fluctuation of height of one mass peak of TOF mass spectrometer becomes acceleratively remarkable as the concentration of that species is reduced, especially serious in the measurement of highly diluted atom amount as in the present case even when the pressure of the ion source and the trap current are kept as high as possible. Furthermore, in order to avoid the fragmentation peaks of the molecules coexisting in quantities the electron acceleration potential should be reduced to the lowest level, which makes the situation quite worse. Therefore, one is forced to take a statistical average of a number of repeated observations.

One way of accomplishing this, attempted here, is the densitometric determination of the most probable peak height in the photogram taken as the superpose of wide-spreading peak tops exposed for hundreds repetitions of oscilloscope displays, where only the top of the peak is brightened using a narrow ( $20 \text{ nsec}$ ) unblanking gate pulse drawn out of the analog output system. Fig. 4 is a schematic representation of the photogram obtained in the experiment given below (blackness is replaced by breadth).

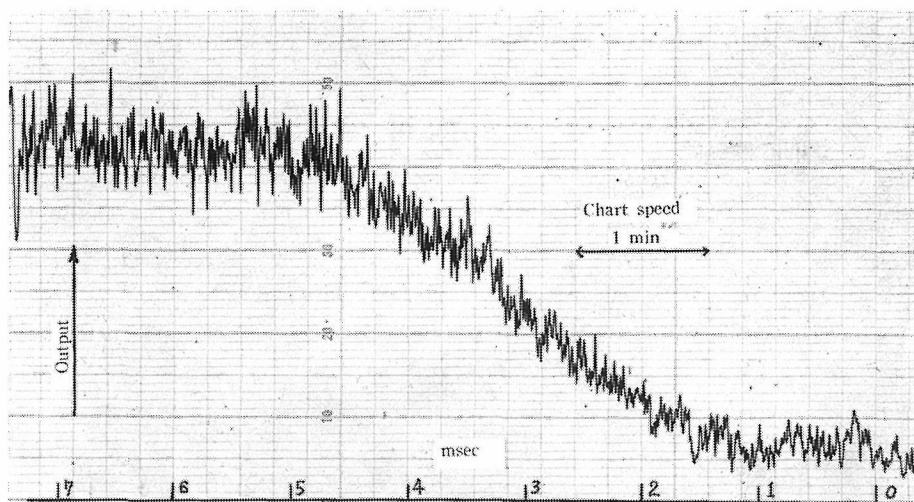


Fig. 5. Pen-record of atom concentration profile.

Another method used by us is to write, on a pen recorder, the mean output of peak pulses picked up by gate mechanism at one fixed position of the horizontal sweep on the oscilloscope after smoothed with a large time constant (say,  $2 \text{ sec}$ ), the position on the time axis being successively shifted automatically. Here, as is seen in Fig. 5, the fluctuation is still rather large, especially for high output.

In some cases a condenser with large capacity was charged with the above-

## Determination of Micro-reactor Volume by TOF Mass Spectrometer

mentioned pulses for a fixed duration (2 min) at each peak position and the produced potential difference was measured; but even by this integration method the precision could not be much improved.

### III. APPLICATION TO THE REACTION $O + NO_2 \rightarrow O_2 + NO$

#### Conditions of the present experiment

##### 1. Raw materials

Argon carrier gas purity 99.99%; oxygen (99.4%) was purified with heated copper oxide, soda lime and  $P_2O_5$ ;  $NO_2$  was purified by repeated bulb-to-bulb distillations after degassing the solid at  $-30^\circ C$  by vacuum, and stored at 70 mmHg. NO and  $N_2O$  were absent as estimated by gas chromatography.

##### 2. Dimensions of the reaction system

Diameter of the flow tube of O atom-carrier gas 0.58 cm, distance from the M.W. cavity to the inlet of the reactor 16.5 cm; reactor diameter 1.6 cm and the nominal inner volume 1.79 cc; leak pin hole diameter 0.05 mm on a teflon-coated gold foil; distance between the reactor and the pin hole 0.2 cm.

##### 3. Flow conditions

Ar + (0.1-0.8%)  $O_2$  0.9-4.4 NPcc/sec; 6-100%  $NO_2$ -Ar mixture 0.01-1 NPcc/sec; pressures, at the cavity 2.3-6.2 mmHg, at the inlet of the reactor 2.0-5.7 mmHg, in the reactor 0.6-2.6 mmHg; mean linear speed in the flow tube 1100-2200 cm/sec, time of passage 7-16 msec, and residence time in the reactor 0.9-2.4 msec; approximate O atom concentration  $(O)/(O_2)$  0.36 as determined by  $NO_2$  titration; ambient temperature  $30^\circ C$ , and in the reactor same as the ambient during the reaction (obs.).

##### 4. Operation condition of the TOF mass spectrometer

Ion source pressures, back ground  $4 \times 10^{-7}$  mmHg, during the observation *ca.*  $8 \times 10^{-6}$  mmHg, operation cycle 40 kc; electron pulse width 1.4  $\mu$ sec; trap current 2  $\mu A$ ; accelerating potential 23 eV (nominal), or 17.9 eV as calibrated by Ar.

##### 5. Discharge conditions

2450 Mc, cycle of discharge 20  $sec^{-1}$ , duty 1/2 and input 100 w.

#### Examination of the experimental conditions

The features of the present experiment is almost the same as reported by Phillips,<sup>3)</sup> Klein<sup>4)</sup> and Clyne,<sup>5)</sup> so only the conclusions will be summarized without detailed discussions.

##### 1. Radial distribution of O atoms in the flow tube

Sample calculation on the distribution of atoms in the sectional plane of the tube with the equation for impermeable circular wall<sup>6)</sup> with  $D' = 270$   $cm^2 \cdot mmHg / sec$  given by Kaufman<sup>7)</sup> for O atoms in  $O_2$  gives that the atoms confined initially in the central area 2.8% of the total cross section will diffuse homogeneously (within 10% deviation) in 0.1 msec, which, when compared with the total transit

time  $>7$  msec, is sufficient to remove the radial distribution of atom concentration due to the radial velocity gradient in the flow of the carrier gas, evidently laminar under the present condition.

## 2. Species produced by M.W. discharge

A number of papers have been presented on this problem<sup>8,8-16</sup>; it seems almost certain from the survey of them that the produced O atoms are solely in the ground  $^3P$  state, not in  $^1D$  or  $^1S$ , and a fair amount of excited  $O_2$  in  $^1\Delta_g$ , along with slight  $^1\Sigma_g^+$ , must be present, but they are not vibrationally excited. However, these excited oxygen will not react with  $NO_2$ .<sup>14</sup>

## 3. O atom loss due to wall recombination

When the recombination coefficient on pyrex glass is taken to be  $2 \times 10^{-5}$  as given by Kaufman,<sup>12</sup> the loss is calculated to be at most 0.7% in the flow tube and 0.04% in the reactor under the prevailing condition.

## 4. O atom loss due to gas phase recombination

Using  $k = 6 \times 10^8$  l<sup>2</sup>/mole<sup>2</sup>·sec of Campbell<sup>17</sup> for  $2O + Ar \rightarrow O_2 + Ar$  we get the loss less than  $10^{-3}$  in the flow tube and in the reactor.

## 5. O atom loss due to ozone formation

The rate constant of ozone formation  $O(^3P) + O_2 + Ar \rightarrow O_3 + Ar$  ( $k_1$ ) has been given by Clyne<sup>13</sup> to be  $1.8 \times 10^8$  l<sup>2</sup>/mole<sup>2</sup>·sec, and in order to estimate the upper limit of O atom decay we consider only the reaction  $O + O_3 \rightarrow 2O_2$  ( $k_2$ ) though it has been stated that ozone is also destroyed by  $O_2^*(+O_3 \rightarrow O(^3P) + 2O_2)$ ,<sup>13-16,18,19</sup> then the loss becomes less than 0.4% in the flow tube and much smaller in the reactor. Further, the maximum steady concentration of ozone is given by  $(O_3)/(O)_0 = 3\%$  using  $k_1/k_2 = 50$  l/mole.<sup>18</sup>

## 6. Correction for $NO_2$ flow rate caused by the equilibrium $N_2O_4 \rightleftharpoons 2NO_2$

In the storage at 30°C and 70 mmHg  $N_2O_4$  is 24.6% of the total gas ( $k_p = 0.213$  in atm<sup>20</sup>), and at the point of mixing where the partial pressure is less than 0.07 mmHg  $N_2O_4$  should be completely dissociated. Accordingly the molal flow rate of  $NO_2$  into the reactor should be 1.25 times that of equilibrium mixture measured at 70 mmHg. The rate constant of  $N_2O_4 + M \rightarrow 2NO_2 + M$  is  $2.57 \times 10^8$  l/mole·sec at 30°C<sup>21</sup> and since the time spent between the reducing valve and the reactor is more than 1 sec, the residual amount of  $N_2O_4$  is only one  $10^{18}$ th of  $NO_2$  at the inlet of the reactor.

## 7. Neglect of $O + NO + M \rightarrow NO_2 + M$ and $O + NO \rightarrow NO_2 + h\nu$

As is well known, these rate constants (*ca.*  $3 \times 10^{10}$  l<sup>2</sup>/mole<sup>2</sup>·sec<sup>4,12,22,26</sup>)  $\times 9.1 \times 10^{-5}$  mole/l, and  $1.5 \times 10^4$  l/mole·sec,<sup>12,22</sup> respectively) are negligibly smaller than the reported rate constant of the first step  $O + NO_2 \rightarrow O_2 + NO$  ( $k \approx 3 \times 10^9$  l/mole·sec, see later).

## Results and Discussion

In Fig. 6-a is given an example of the concentration profile at the end of



the flow tube, where the micro-reactor is not attached and the tube opening lies 0.2 cm apart from the pin hole.

The originally sharp front now assumes a S-curve having the rise time of about 2 msec owing to axial diffusion. The diffusion parameter  $\chi$  which fits the observed curve is somewhat larger than the upper limit of the calculated from the quantities given in the figure. However, in this calculation the radius of pipe affects the result by the third power, and the diffusion coefficient  $D'$  is assumed to be 270 cm<sup>2</sup>·mmHg/sec as cited before<sup>7)</sup> without correction for the change from O<sub>2</sub> to Ar and there is another determination,  $D'=240$  at 27°C in O<sub>2</sub>,<sup>27)</sup> therefore some ambiguity must remain in the value used; further there may be uncalculable effect of the flow turbulence in the space between the tube opening and the pin hole, so we are to use the  $D'/r^3$  derived from this observed  $\chi$  as an experimental constant in the next step.\*

Fig. 6-b is an example of estimating effective volume of the reaction zone taken from the exp. no. 16 of Table 1. As is seen in the figure it is impossible to determine this volume within 0.1 cc (*i.e.*  $\pm 5\%$ ). However, the obtained volume seems a little larger than the nominal value and remains constant in 9 sets of conditions covering the entire flow range, suggesting invariability of the efficacy of mixing and the complete mass mixing within the flow condition experimented.

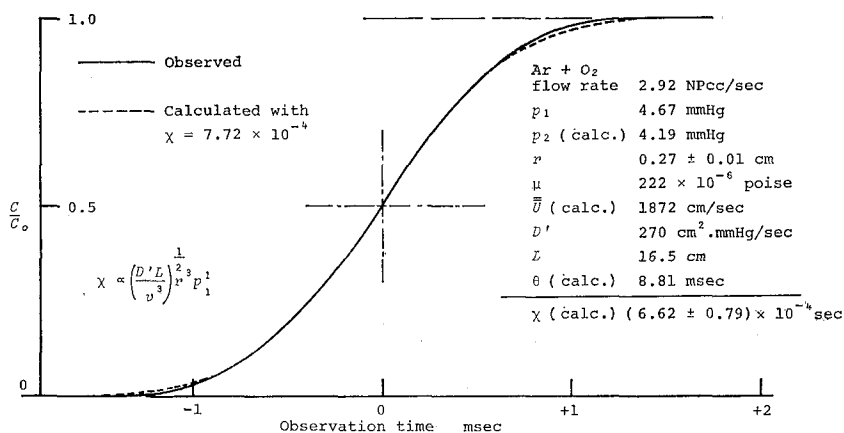
The ratio  $C/C_0$  of O atom used here is the output ratio of  $M/e=16$  peak itself with the correction of the fragmentation of O<sub>2</sub> and back ground H<sub>2</sub>O; the assumption of linearity between the output and the partial pressure of O atoms in front of the pin hole is presumably correct as judged from the pressure in front of the leak and its hole diameter and the low output of mass peak. The time interval of mass spectrometer pulse has been calibrated accurately by an electronic pulse counter, and the pressure or the flow rate measurement is correct within 0.4% or 2%, respectively.

\* There must be a doubt that the sharpness of the front of discharge input does not necessarily assure the sharp front of the produced atom bunch since the discharge zone has some length. The equation corresponding to (I) derived from the assumption that the atom concentration increases linearly through the entire discharge zone from 0 to  $C_0$  is expressed by

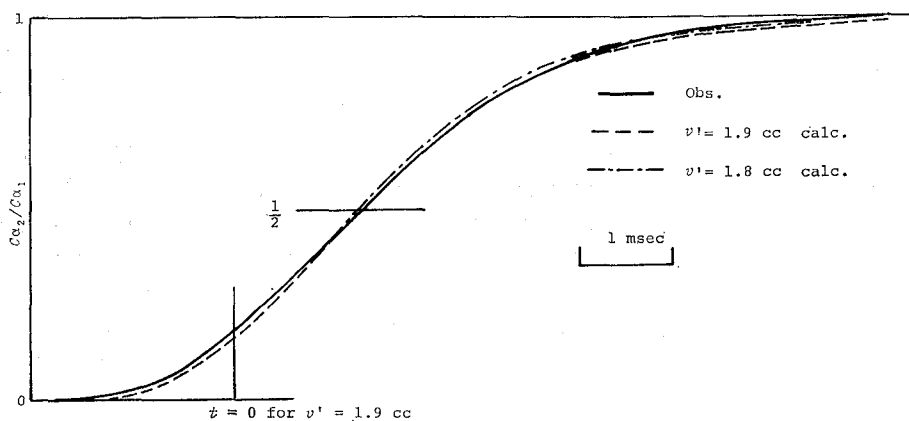
$$\frac{C}{C_0} = \frac{1}{2} \left\{ \frac{\sqrt{4D\theta/\pi}}{l} \left[ \exp\left(-\frac{t^2}{\chi^2}\right) - \exp\left(-\left[-\frac{t}{\chi} + \frac{\tau}{\chi'}\right]^2\right) \right] + \left[ \frac{t\bar{U}}{\tau U'} - 1 \right] \operatorname{erf}\left(-\frac{t}{\chi} + \frac{\tau}{\chi'}\right) + 1 + \left[ \frac{t\bar{U}}{\tau U'} \right] \operatorname{erf}\left(\frac{t}{\chi}\right) \right\}$$

where  $l$  length of discharge zone  $\times$  {sectional area of flow pipe at the cavity}  $\div$  {sectional area of the inlet pipe},  $\tau$  residence time in the discharge,  $U'$  linear speed in the inlet pipe at the outlet of cavity and  $\chi' = \sqrt{4D\theta/U'}$ . A sample calculation with the conditions given in Fig. 3-a and the discharge zone 5 cm (=slot width of cavity;  $\tau=7.9$  msec) gives the similar curve with the rise time 6.4 msec from  $C/C_0=0.05$  to 0.95, which differs by far from the observed one (1.7 msec).

Therefore, rather conversely speaking, the good coincidence between the observed curve and the calculated by (I) seems to suggest that the concentration of atoms reaches its final value within a very short first portion of the discharge independent of the succeeding discharge length.



a) Concentration profile at the end of flow tube without micro-reactor, showing axial diffusion



b) With micro-reactor and without second reactant

Fig. 6. Determination of diffusion parameter and the reaction volume.

Experimental results are tabulated in Table 1; the range of conditions is not so wide, *i.e.* the flow rate of O-carrier gas varies 5-fold and that of NO<sub>2</sub>-Ar 10-fold, and the NO<sub>2</sub> concentration into the reactor is 6-100% and initial NO<sub>2</sub> concentration in the reactor is 0.3-1.7 mole/l, O<sub>2</sub> concentration in the inflowing gas is 0.15-0.8% and O concentration in the reactor is (0.5-1.2) × 10<sup>-7</sup> mole/l. The speed in the flow tube lies in 11-22 m/sec (transit time 7-16 msec) and the residence time in the reactor varies from 0.9 to 2.4 msec at 2-5.7 mmHg. Further, the extent of conversion of O or NO<sub>2</sub> is 49-91% or 6-55%, respectively.

In the determination of C'/C<sub>0</sub> by the output of M/e=16 during the reaction, correction has been made of the fragmentation of NO<sub>2</sub>, and the peak height of M/e=46 for NO<sub>2</sub> has been calibrated by known sample.

Nevertheless, scatter in the observed rate constants is rather large even at one fixed O<sub>2</sub>-Ar gas flow as given in Fig. 7, and some trend may be seen with respect to Ar-O<sub>2</sub> flow rate in the experiments with high NO<sub>2</sub> concentration (Fig. 7-a), but with the lower NO<sub>2</sub> concentration no dependence is found on the varia-

Table 1. Experimental results at 30°C.

Exp. No.	Dilut. of NO <sub>2</sub> $\frac{\text{NO}_2}{\text{NO}_2+\text{Ar}}$	Dilut. of O <sub>2</sub> $\frac{\text{O}_2}{\text{Ar}} \times 10^4$	Ar+O <sub>2</sub> flow rate $\frac{\text{NPcc}}{\text{sec}}$	Press. at the cavity $p_1$ mmHg	Press. before reactor $p_2$ mmHg	Mean speed $U$ cm/sec	Transit time $\theta \times 10^3$ sec	Ar+NO <sub>2</sub> flow rate $\frac{\text{NPcc}}{\text{sec}}$	Press. in the reactor $p_r$ mmHg	$\lambda \times 10^3$ sec	Reaction volume $v'$ cc	Residence time $10^3/\alpha_2$ sec	In the reactor				$k_{\text{app}} \times 10^{-9}$ l/mole·sec (maximum deviation)		
													$\frac{(\text{O})_0}{\times 10^{17}}$ mole/l	$\frac{(\text{NO}_2)_0}{\times 10^6}$ mole/l	$\frac{(\text{O})/(\text{O})_0}{C/\alpha_2/C_0\alpha_1}$	$\frac{(\text{NO}_2)}{(\text{NO}_2)_0}$			
1								0.20	2.32		1.9±0.1		0.322	0.44	0.81	3.7			
2		15	4.3+0.0066	6.04	5.48	2118	7.80	0.25	2.34	0.571	(1.9)	1.29	0.66	0.395	0.37	0.83	4.1	4.0(±1.3)	
3								0.40	2.40		1.9±0.1			0.631	0.22	0.82	5.4		
4								0.74	2.62		(1.9)			1.18	0.22	0.82	2.9		
5								0.21	1.86		1.9±0.1	1.43		0.375	0.32	0.80	5.0		
6								0.39	1.92		(1.9)	1.41		0.669	0.22	0.80	4.7	3.8(±1.2)	
7		22	3.0+0.0066	4.91	4.42	1840	8.97	0.57	2.02	0.782	(1.9)	1.40	0.73	1.00	0.26	0.75	2.8		
8								0.72	2.09		(1.9)	1.40		1.23	0.22	0.76	2.8		
9								1.03	2.21		1.9±0.1	1.36		1.72	0.13	0.78	3.6		
10	0.057							0.49	1.71		(1.9)	1.51		0.79	0.896	0.27	0.76	2.5	3.4(±1.4)
11		29	2.3+0.0066	4.20	3.75	1674	9.86	0.55	1.74	0.977	1.9±0.1	1.50		0.78	1.01	0.22	0.75	3.1	
12								0.71	1.79		(1.9)	1.46		0.76	1.28	0.13	0.75	4.7	
13								0.17	1.31		1.9±0.1	1.69		0.85	0.354	0.34	0.71	4.7	4.6(±0.6)
14		37	1.8+0.0066	3.64	3.25	1459	11.3	0.28	1.37	1.29	(1.9)	1.67		0.85	0.563	0.26	0.75	4.1	
15								0.41	1.41		(1.9)	1.61		0.82	0.808	0.19	0.73	4.4	
16								0.53	1.47		1.9±0.1	1.59		0.81	1.04	0.14	0.74	5.2	
17								0.12	0.879		(1.9)	2.19		0.296	0.32	0.64	4.8	5.1(±0.3)	
18		78	0.85+0.0066	2.42	2.13	1069	15.4	0.15	0.851	2.53	(1.9)	2.08	1.1	0.378	0.29	0.60	5.3		
19								0.19	0.838		1.9±0.1	2.10		0.458	0.22	0.70	5.3		

(387)

Determination of Micro-reactor Volume by TOF Mass Spectrometer

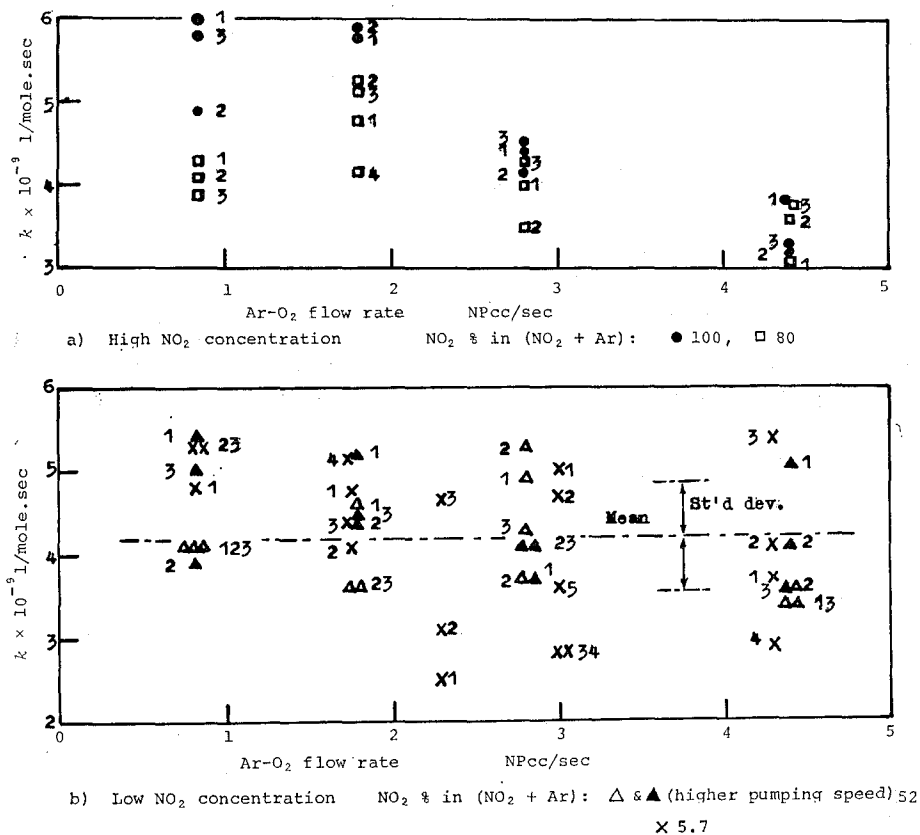
20														0.438	0.38	0.80	3.4		
21		15	4.4+0.0067	6.19	5.63	2124	7.77	0.040	2.40	0.560	(1.9)	1.34	0.69	0.587	0.29	0.88	3.6	3.5(±0.1)	
22								0.054						0.801	0.23	0.92	3.4		
23								0.068						0.999	0.19	0.93	3.4		
24								0.030						0.292	0.50	0.77	5.1		
25		‡15	4.4+0.0067	5.94	5.35	2226	7.40	0.056	1.57	0.535	1.9±0.1	0.875	0.48	0.539	0.40	0.86	3.6	4.3(±0.8)	
26								0.071				0.872		0.678	0.32	0.89	4.1		
27								0.019						0.337	0.41	0.58	4.9		
28								0.020						0.318	0.33	0.79	5.3	4.6(±0.9)	
29		24	2.8+0.0067	4.58	4.10	1815	9.09	0.033	1.69	0.828	(1.9)	1.51	0.78	0.545	0.29	0.82	3.7		
30								0.046						0.758	0.19	0.90	4.3		
31								0.033				1.01		0.358	0.51	0.72	3.7		
32		0.52	‡24	2.8+0.0067	4.40	3.90	1900	8.70	0.046	1.13	0.791	(1.9)	0.993	0.55	0.506	0.40	0.72	4.1	4.0(±0.3)
33								0.059					1.00	0.643	0.32	0.82	4.1		
34								0.019						0.389	0.33	0.62	4.6		
35								0.032						0.676	0.25	0.69	3.6	3.9(±0.7)	
36			38	1.8+0.0067	3.63	3.24	1450	11.4	1.29	1.30	(1.9)	1.83	0.94	1.12	0.14	0.82	3.6		
37								0.021						0.284	0.51	0.53	5.2		
38								0.027						0.482	0.38	0.63	4.4	4.7(±0.5)	
39			‡38	1.8+0.0067	3.49	3.09	1516	10.9	0.860	1.25	(1.9)	1.20	0.66	0.844	0.22	0.77	4.5		
40								0.017	0.788			2.34		0.449	0.25	0.69	4.1		
41								0.022	0.788	2.53	(1.9)	2.33	1.2	0.571	0.21	0.69	4.1	4.1(±0.0)	
42			80	0.83+0.0067	2.35	2.06	1080	15.3	0.804			2.36		1.03	0.11	0.82	4.1		
43								0.033						0.563	0.28	0.54	5.4		
44								0.049	0.547	2.35	(1.9)	1.51	0.86	0.806	0.25	0.63	3.9	4.8(±0.9)	
45			‡78	0.85+0.0067	2.27	1.96	1138	14.5	0.061			1.50		1.01	0.15	0.75	5.0		

46							0.018						0.397	0.39	0.83	3.6		
47		15	4.4+0.0067	6.07	5.50	2170	7.60	0.030	2.36	0.548	(1.9)	1.33	0.68	0.668	0.29	0.90	3.1	3.5(±0.4)
48								0.039						0.870	0.20	0.92	3.8	
49								0.013						0.323	0.43	0.68	4.0	
50		24	2.8+0.0067	4.58	4.10	1815	9.09	0.019	1.70	0.828	(1.9)	1.53	0.78	0.483	0.32	0.83	3.5	3.9(±0.4)
51								0.028						0.726	0.19	0.90	4.3	
52	0.80							0.011						0.343	0.35	0.74	4.2	
53		36	1.9+0.0067	3.64	3.23	1533	10.8	0.015	1.31	1.20	(1.9)	1.75	0.90	0.444	0.24	0.80	5.2	4.9(±0.7)
54								0.019						0.571	0.18	0.84	5.3	
55								0.025						0.737	0.14	0.86	4.8	
56								0.0098				2.43		0.409	0.30	0.61	3.9	
57		80	0.84+0.0067	2.39	2.10	1066	15.5	0.014	0.822	2.56	(1.9)	2.42	1.2	0.577	0.20	0.69	4.1	4.1(±0.2)
58								0.029				2.38		1.18	0.09	0.82	4.3	
59								0.014						0.400	0.38	0.83	3.8	
60		15	4.4+0.0067	6.23	5.67	2115	7.80	0.030	2.39	0.562	(1.9)	1.34	0.69	0.854	0.23	0.91	3.2	3.4(±0.4)
61								0.039						1.11	0.18	0.94	3.3	
62								0.013						0.425	0.30	0.80	4.4	
63		24	2.8+0.0067	4.65	4.18	1784	9.25	0.021	1.73	0.842	(1.9)	1.55	0.79	0.700	0.20	0.88	4.2	4.4(±0.2)
64	1.00							0.025						0.833	0.16	0.91	4.5	
65								0.0077						0.295	0.33	0.66	5.8	
66		37	1.8+0.0067	3.71	3.32	1482	11.1	0.011	1.32	1.25	(1.9)	1.78	0.91	0.430	0.24	0.69	5.9	5.9(±0.1)
67								0.0070						0.349	0.32	0.45	6.0	
68		77	0.87+0.0067	2.40	2.10	1105	14.9	0.011	0.820	2.42	(1.9)	2.30	1.2	0.558	0.18	0.70	4.9	5.6(±0.7)
69								0.015						0.737	0.12	0.79	5.8	

$v'$  is determined by the given condition but  $\text{NO}_2$ ;  $v'$  in parentheses is the assumed value.

\* At higher pumping speed. \* Rough estimate assuming  $\text{O}/\text{O}_2=0.36$  throughout.

$D'=270 \text{ cm}^2\cdot\text{mmHg}/\text{sec}$ ,  $\mu_{\text{Ar}}=2.29\times 10^{-8}$  poise.



Number by the point represents the increasing order of NO<sub>2</sub>-Ar flow rate in each series.

Fig. 7. Plot of the observed rate constants of O+NO<sub>2</sub> at 30°C.

tion of any specified condition, so the homogeneity the reaction must have been retained within the flow speed of the second reactant used here at least with the dilute NO<sub>2</sub>.

Thus, the most part of the source of error must lie in the accuracy of TOF mass spectrometric ratio determinations (usually ±10%) which affects largely

Table 2. Comparison with the reported values.

Rate Const. $k \times 10^{-9}$ l/mole·sec	Method	Temp.	Author
>1	flash photolysis of NO <sub>2</sub> , mass spectr.	(room)	Kistiakowsky, 1957 <sup>29)</sup>
≥1	(N+NO)+NO <sub>2</sub> , mass spectr.	room	Kistiakowsky, 1957 <sup>1)</sup>
2.1	NO <sub>2</sub> photolysis, photometry	27°C	Ford, 1957 <sup>23)</sup>
≈1	(M.W. on O <sub>2</sub> )+NO <sub>2</sub> , chemilumi.	room	Kaufman, 1959 <sup>26)</sup>
1.5±0.4	(M.W. on O <sub>2</sub> )+NO <sub>2</sub> , mass spectr.	25°C	Phillips, 1962 <sup>3)</sup>
3.4	recalc. of ref. 23)	27°C	Benson, 1963 <sup>28)</sup>
3.28±0.33	(N+NO)+NO <sub>2</sub> , mass spectr.	25°C	Klein, 1964 <sup>1)</sup>
4.18±0.64 (standard deviation)	(M.W. on O <sub>2</sub> )+NO <sub>2</sub> , mass spectr.	30°C	This work

(up to  $\pm 40\%$ ) the calculation of  $k$  in eq. 4.

The mean value of observed 45  $k$ 's in the experiments with  $(\text{NO}_2) \leq 52\%$  is  $\{4.18 \pm (\text{standard deviation } 0.64)\} \times 10^9$  l/mole·sec at  $30^\circ\text{C}$  which is in fair agreement with the reported values as given in Table 2.

#### IV. APPLICATION TO THE REACTION $\text{N} + \text{NO} \rightarrow \text{N}_2 + \text{O}$

##### Experimental conditions

The items of experimental condition are the same as in III unless otherwise stated.

##### 1. Raw material

In this experiment N atoms have been produced in the pure (99.999%)  $\text{N}_2$  stream since the N concentration in  $\text{N}_2$  is low enough ( $\text{N}/\text{N}_2$  obs. = 1%) and the addition of inert gas must cause an appreciable formation of excited metastable atoms.<sup>30)</sup>

Cylinder NO (99.0%, 0.1%  $\text{NO}_2$ , remainder  $\text{N}_2$ ) was used without further purification.

##### 2. Flow conditions

$\text{N}_2$  0.90–4.5 NPcc/sec, mean linear speed in the flow tube 1300–2200 cm/sec, time of passage 12.7–7.5 msec; 12–100% NO-Ar mixture 0.0047–0.076 NPcc/sec, pressure in the reactor 0.47–1.67 mmHg; residence time in the reactor 0.89–1.36 msec; ambient temperature  $25^\circ\text{C}$ .

##### 3. Species produced by M.W. discharge

It must be sufficient to cite two literatures<sup>30,31)</sup> as to the species present in active nitrogen: in the discharged pure nitrogen of low pressure most part of N atoms lie in the ground  $^4\text{S}$  state, and atoms in  $^2\text{D}$  and  $^2\text{P}$  states must be less than 1% which are quite easily deactivated downstream; further, vibrationally excited, both ground and metastable  $\text{A}^3\Sigma_u^+$  states, molecules have been reported to be present,<sup>30)</sup> the latter can survive for some msec.

##### 4. Temperature rise in the reactor

In contrast to the case of O atom, the temperature of the reactor wall (as supposed from the slowness of rise or fall of the temperature measured by a fine thermocouple inserted in the gaseous space but not perfectly thermally isolated from the wall) increased much higher than the ambient ( $30$ – $98^\circ\text{C}$  according to the flow condition) when the discharged nitrogen passed through the reactor and the admission of NO in the reactor did not alter this temperature rise entirely. Since the recombination rate of N atoms does not differ appreciably from that in O-Ar flow described before, the cause of this exothermicity should be sought in other phenomena; supposingly the dissipation of excess energy at the wall of the metastable and/or highly excited vibrational states of  $\text{N}_2$  may account for this.

Fortunately, the reaction  $\text{N} + \text{NO}$  has a very low activation heat ( $200 \pm 700$  cal/mole<sup>32)</sup>) and the rate constant has been reported to be practically independent

Table 3. Experimental results on N+NO.

Exp. No.	Dilut. of NO $\frac{\text{NO}}{\text{NO}+\text{Ar}}$	$\text{N}_2$ flow rate NPcc/sec	Press. at the cavity $p_1$ mmHg	Ar+NO flow rate NPcc/sec	Press. in the reactor $p_r$ mmHg	Residence time $10^3/\alpha_2$ sec	In the reactor				$k \times 10^{-10}$ l/mole $\cdot$ sec	$k_{\text{av}} \times 10^{-10}$ (maximum deviation) l/mole $\cdot$ sec
							$(\text{N})_0$ $\times 10^7$ mole/l	$(\text{NO})_0$ $\times 10^7$ mole/l	$(\text{N})/(\text{N})_0$	$(\text{NO})/(\text{NO})_0$		
1				0.039		1.41		1.22	0.54	0.44	1.13	
2		0.85	2.10	0.052	0.501	1.39	2.0	1.60	0.41	0.47	1.38	1.24( $\pm 0.14$ )
3				0.076		1.35		2.30	0.37	0.45	1.22	
4				0.040				1.17	0.74	0.28	0.98	
5	0.122	1.78	3.29	0.056	0.813	1.11	3.2	1.61	0.67	0.31	0.88	0.97( $\pm 0.09$ )
6				0.063				1.82	0.60	0.32	1.04	
7				0.044				1.11	0.80	0.18	1.30	
8		2.98	4.57	0.060	1.18	0.97	4.4	1.52	0.72	0.24	0.95	1.11( $\pm 0.29$ )
9				0.073				1.83	0.69	0.24	1.08	
10				0.017		1.36		1.24	0.73	0.23	0.96	
11		0.90	2.20	0.024	0.499	1.35	2.9	1.77	0.55	0.26	1.36	1.17( $\pm 0.20$ )
12				0.034		1.34		2.44	0.44	0.32	1.20	
13				0.036		1.09		2.34	0.61	0.27	1.01	
14	0.254	1.77	3.24	0.047	0.786	1.08	4.0	2.77	0.52	0.30	1.04	1.03( $\pm 0.02$ )
15				0.043				2.25	0.72	0.23	0.80	
16		3.04	4.67	0.061	1.20	0.97	5.4	3.11	0.57	0.25	0.99	1.04( $\pm 0.20$ )
17				0.027				1.40	0.72	0.21	1.34	
18				0.050				2.42	0.74	0.18	0.87	
19		4.50	6.10	0.023	1.67	0.92	7.0	1.11	0.86	0.16	1.01	0.94( $\pm 0.10$ )

Yoshinasa TAKEZAKI and Sadayuki MORI



20			0.020		1.37		2.88	0.37	0.38	1.14		
21		0.90	2.21	0.012	0.505	1.38	2.7	1.71	0.56	0.30	1.14	1.17( $\pm 0.07$ )
22				0.026		1.36		3.78	0.24	0.49	1.25	
23				0.019				2.21	0.56	0.27	1.17	
24		1.77	3.23	0.028	0.782	1.09	3.8	3.22	0.44	0.33	1.11	1.10( $\pm 0.10$ )
25	0.50			0.035				4.04	0.36	0.39	1.02	
26				0.020				2.03	0.68	0.22	1.10	
27		2.93	4.50	0.029	1.16	0.98	4.9	3.05	0.54	0.26	1.12	1.04( $\pm 0.13$ )
28				0.039				4.03	0.47	0.32	0.91	
29				0.026				2.54	0.67	0.17	1.23	
30		4.45	5.98	0.039	1.64	0.91	6.6	3.79	0.56	0.24	0.96	1.05( $\pm 0.18$ )
31				0.057				5.52	0.43	0.28	0.95	
32				0.005		1.30		1.29	0.66	0.23	1.32	
33		0.90	2.13	0.011	0.469	1.29	2.8	2.98	0.33	0.45	1.17	1.19( $\pm 0.13$ )
34				0.007		1.29		1.93	0.53	0.33	1.07	
35				0.007				1.71	0.63	0.25	1.25	
36		1.78	3.25	0.012	0.782	1.09	4.3	2.84	0.55	0.31	0.88	0.97( $\pm 0.23$ )
37	1.00			0.023				5.39	0.34	0.44	0.77	
38				0.011				2.49	0.67	0.27	0.68	
39		2.72	4.50	0.018	1.14	1.04	5.6	3.98	0.58	0.32	0.54	0.61( $\pm 0.07$ )
40				0.023				5.16	0.45	0.37	0.63	
41				0.016				2.96	0.58	0.28	0.96	
42		4.48	6.00	0.021	1.61	0.89	6.2	3.98	0.55	0.31	0.74	0.82( $\pm 0.14$ )
43				0.027				5.08	0.45	0.36	0.76	

Reaction volume  $v'$  is taken to be 1.9 cc as in III.

of temperature between 203–478°C<sup>32)</sup>, therefore, no special correction has been made on the observed rate constant.

##### 5. Neglect of $O+NO+M \rightarrow NO_2+M$ and $O+NO \rightarrow NO_2+h\nu$ as NO-competing reactions

As stated in III these rate constants are much smaller than that of  $O+NO_2$  which is still about ten times slower than  $N+NO$  (see later).

### Results

The results obtained in the same reactor system as before are reproduced in Table 3 and Fig. 8.

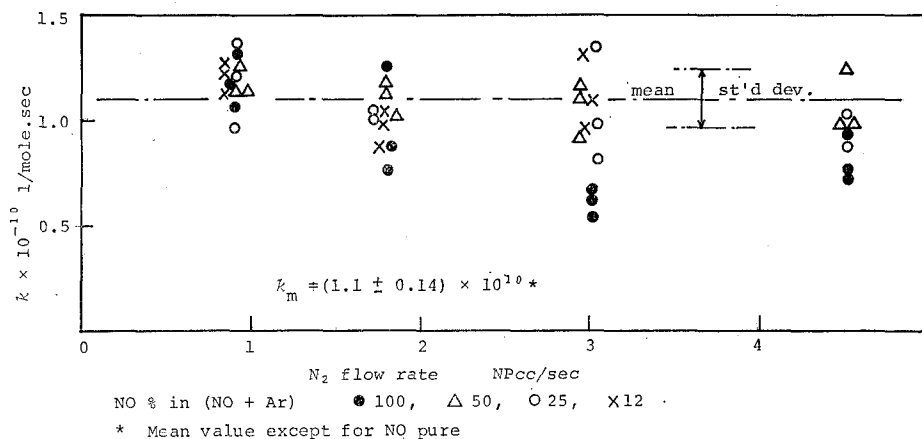


Fig. 8. Plot of the observed rate constants of  $N+NO$  at room temperature.

The mean value of observed 21  $k$ 's in the experiments except those with  $NO$  pure is  $(1.1 \pm 0.14) \times 10^{10}$  l/mole·sec, which is in fair agreement with the reported figures,  $(1.3 \pm 0.36) \times 10^{10}$  l/mole·sec obtained by Phillips and Schiff<sup>3)</sup> and  $2.2 \times 10^{10}$  by Clyne and Thrush,<sup>32)</sup> but is less than the lower limit of approximate estimation,  $5 \times 10^{10}$ , made by Kistiakowsky and Volpi.<sup>1-b)</sup>

Thus, although the obtained result is by no means satisfactory for the precise determination at present and needs further refinements, this procedure would be expected to be a useful method for the determination of very fast reaction rate constant.

Thanks are due to the grant of the Ministry of Education (1963) for installing TOF mass spectrometer.

### REFERENCES

- (1) G. B. Kistiakowsky and G. G. Volpi, *J. Chem. Phys.*, 27, 1141 (1957) and 28, 665 (1958).
- (2) E. W. Wong and A. E. Potter, Jr., *ibid.*, 39, 2211 (1963).
- (3) L. F. Phillips and H. I. Schiff, *ibid.*, 36, 1509 (1962).
- (4) F. S. Klein and J. R. Herron, *ibid.*, 41, 1285 (1964).
- (5) M. A. A. Clyne and B. A. Thrush, *Trans. Faraday Soc.*, 58, 511 (1962).
- (6) J. Kranck, "The Mathematics of Diffusion," p. 76, Oxford (1956).
- (7) F. Kaufman, "Progress in Reaction Kinetics I," Ed. Porter, p. 13, Pergamon, (1961).
- (8) J. W. Linnett and D. G. H. Marsden, *Proc. Royal Soc. (London)* A234, 489 (1956).

Determination of Micro-reactor Volume by TOF Mass Spectrometer

- (9) L. Elias, E. A. Ogryzlo and H. I. Schiff, *Can. J. Chem.*, **37**, 1680 (1959).
- (10) J. T. Herron and H. I. Schiff, *ibid.*, **36**, 1159 (1958).
- (11) S. N. Foner and R. L. Hudson, *J. Chem. Phys.*, **25**, 601 (1956).
- (12) F. Kaufman, *Proc. Royal Soc. (London)*, **A247**, 123 (1958).
- (13) M. A. A. Clyne, D. T. McKenney and B. A. Thrush, *Trans. Faraday Soc.*, **61**, 2701 (1965).
- (14) L. W. Bader and E. A. Ogryzlo, *Disc. Faraday Soc.*, **37**, 46 (1964).
- (15) F. Kaufman and J. R. Kelso, *ibid.*, **37**, 26 (1964).
- (16) M. A. A. Clyne, B. A. Thrush and R. P. Wayne, *Nature*, **199**, 1057 (1963).
- (17) I. M. Campbell and B. A. Thrush, *Proc. Royal Soc. (London)*, **A296**, 222 (1967).
- (18) A. Mathias and H. I. Schiff, *Disc. Faraday Soc.*, **37**, 38 (1964).
- (19) P. Harteck and R. R. Reeves, Jr., *ibid.*, **37**, 82 (1964).
- (20) Landoldt-Börnstein, "Phys. Chem. Tabellen II," s. 1418, Julius Springer, (1923).
- (21) T. Carrington and N. Davidson, *J. Phys. Chem.*, **39**, 418 (1953).
- (22) F. Kaufman, *J. Chem. Phys.*, **28**, 352 (1958).
- (23) H. W. Ford and N. Endow, *ibid.*, **27**, 1156 (1957).
- (24) P. Harteck, R. R. Reeves and G. Mannella, *ibid.*, **29**, 1333 (1958).
- (25) E. A. Ogryzlo and H. I. Schiff, *Can. J. Chem.*, **37**, 1690 (1959).
- (26) F. Kaufman and J. Kelso, "7th Symposium on Combustion," p. 53, Butterworths, (1959).
- (27) S. Krongelb and M. W. P. Strandberg, *J. Chem. Phys.*, **31**, 1196 (1959).
- (28) S. W. Benson, *ibid.*, **38**, 1251 (1963).
- (29) G. B. Kistiakowsky and P. H. Kydd, *J. Am. Chem. Soc.*, **79**, 4825 (1957).
- (30) S. N. Foner and R. L. Hudson, *J. Chem. Phys.*, **37**, 1662 (1962).
- (31) K. R. Jennings and J. W. Linnett, *Chem. Revs.*, **12**, 116 (1958).
- (32) M. A. A. Clyne and B. A. Thrush., *Proc. Royal Soc. (London)*, **A261**, 259 (1961).